

Inertial Drives for Micro- and Nanorobots: Two Novel Mechanisms

Wolfgang Zesch, Roland Büchi, Alain Codourey, Roland Siegart

Swiss Federal Institute of Technology Zürich ETHZ
Institute of Robotics
CH-8092 Zürich, Switzerland
e-mail: zesch@ifr.mavt.ethz.ch

ABSTRACT

In micro or nanorobotics, high precision movement in two or more degrees of freedom is one of the main problems. Firstly, the positional precision has to be increased (< 10 nm) as the object sizes decrease. On the other hand, the workspace has to have macroscopic dimensions (1 cm^3) to give high manoeuvrability to the system and to allow suitable handling at the micro/macro-world interface. As basic driving mechanisms for the ETHZ Nanorobot Project, two new piezoelectric devices have been developed.

"Abalone" is a 3-dof system that relies on the impact drive principle. The $38\text{ mm} \times 33\text{ mm} \times 9\text{ mm}$ slider can be moved to each position and orientation in a horizontal plane within a theoretically infinite workspace. In the stepping mode it achieves a speed of 1 mm/s in translation and 7 deg/s in rotation. Within the actuator's local range of $6\text{ }\mu\text{m}$ fine positioning is possible with a resolution better than 10 nm . "NanoCrab" is a bearingless rotational micromotor relying on the stick-slip effect. This $10\text{ mm} \times 7\text{ mm} \times 7\text{ mm}$ motor has the advantage of a relatively high torque at low rotational speed and an excellent runout. While the maximum velocity is 60 rpm , it reaches its highest torque of 0.3 mNm at 2 rpm . Another benefit is the powerless holding torque of 0.9 mNm . With a typical step of 0.1 mrad and a local resolution 3 orders of magnitude better than the step angle, NanoCrab can be very precisely adjusted.

Design and measurements of the characteristics of these two mechanisms will be presented and compared with the theoretical analysis of inertial drives presented in a companion paper. Finally their integration into the Nanorobot system will be discussed.

Keywords: inertial drive, impact drive, micropositioning, piezo-electric, positioning table, micromotor

1. INTRODUCTION

In recent years, nano-technology has become an important field of research. Binnig and Rohrer invented the Scanning Tunneling Microscope (STM)¹ to explore the world of atoms and molecules. Other types of probe microscopes like the Atomic Force Microscope (AFM) etc. followed, each of them having sub-nanometer resolution and therefore needing high precision positioning tools. On the other hand micromechanical design, derived from silicon etching technology in microelectronics, has opened a variety of possibilities for new micro and nanosystems. This technology allows the production of microsensors and actuators such as micropressure sensors or electrostatic micromotors in a batch process and is therefore suitable for mass production. Major drawbacks are the limitation to (almost) two dimensional structures and the restriction to a small selection of materials. To overcome these disadvantages and to open new applications, an assembly step, which demands for object handling, has to be introduced to the fabrication process. While this manufacturing operation is already solved in the human sized macro world, it is still the main problem in micro or nanofabrication.

Recognising an increasing demand in automated micro manufacturing devices, the ETH Zürich started a project in 1993 dealing with the development a Nanorobot System². In order to achieve a good performance and to assemble microparts precisely, the manipulation system has to have at least five degrees-of-freedom (dof) and must be able to handle the micrometer sized objects with an accuracy better than 10 nm under a Stereo Scanning Electron Microscope (SSEM). In combination with a vision system the SSEM serves as a position sensor supervising the robot in order to close the control loop. As the sensor system acts completely independent from mechanical hardware, the robot must only have a good mechanical resolution while there is actually no need for an absolute positioning ability. Errors like mechanical tolerances, slow thermal drift, friction effects etc. can therefore be compensated for by the vision feedback control.

The major limitation of the resolution is due to the *stick-slip-effect* resulting from static friction, a finite system stiffness and play in bearings due to manufacturing tolerances. A method resolving the minimal necessary step size is the use of the so called *Inertial Drive*³. This paper focuses on the implementation of the inertial principle of two mechanisms, Abalone, a 3-dof

micropositioning table, and NanoCrab, a micro rotational motor. Using a combination of two different motion modes, these devices are able to achieve nanometer resolution.

The last section then briefly presents an initial implementation of the ETHZ Nanorobot, which already uses the two motors mentioned above.

2. PRINCIPLE OF INERTIAL DRIVE

The physical principle on which inertial drives are based is the same one that allows the "table-cloth-trick" to occur. While a swift pull on a cloth leaves a vase standing on the table at its position, a gentle tug results in the vase's displacement.

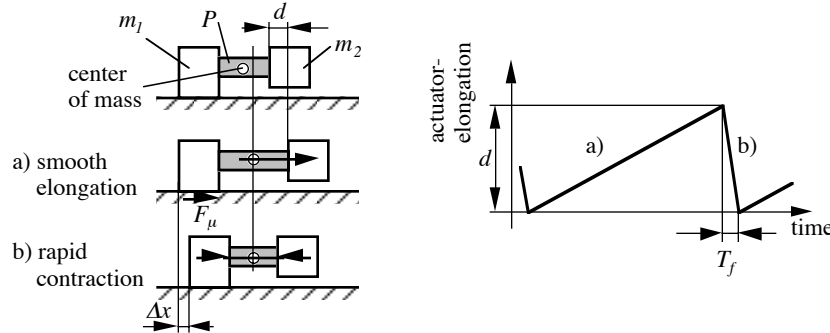


Fig. 1: The inertial drive's principle

To use this effect for micropositioning let us consider a system consisting of two masses m_1 and m_2 connected by a longitudinal actuator P (Fig. 1). Since only m_1 lays on the ground the friction force keeps it from moving during a smooth elongation of P (Fig. 1a). After having reached its final elongation d , P is then rapidly shrunk which induces an inertial force on m_2 . Because this force exceeds the static friction, m_1 moves towards m_2 leading to a net displacement of the complete system. Assuming an ideal sawtooth function for the elongation with an infinitesimal fall time T_f the step size becomes

$$\Delta x = \kappa \cdot d = \frac{m_2}{m_1 + m_2} \cdot d \quad (1)$$

Therefore Δx has an upper bound value d , when the step factor κ tends towards 1 ($m_2 \gg m_1$). For rotations, the masses in (1) have to be replaced by the corresponding inertias

The addition of several of these steps allows a theoretically infinite workspace with very high resolution. Moreover, the minimal step size can even be improved by defining the tool center point (TCP) on m_2 . Smooth control of the actuator leaving m_1 unmoved at its position enables fine positioning. Its resolution, which is determined by the (frictionless) actuator and the electric circuitry only (for piezoelectric elements) reaches the nanometer range.

In the most general form - both m_1 and m_2 non zero - the inertial mechanism is known as an *Impact-Drive*³. If m_1 decreases to zero the step size becomes a maximum ($\kappa = 1$) while the impact on m_2 diminishes to neglectable values. This kind of drive, for which the actuator can even be attached to the ground instead of the moving mass, is called *Stick-Slip-Drive*^{4,5}. Both forms are used in the following sections. A mathematical analysis of the inertial principle can be found in a companion paper⁶.

3. ABALONE - AN XYΘ – MICROPPOSITIONING MECHANISM

Planar positioning of objects requires three dofs, i.e. two translations and one rotation. This task is classically realized by stacking three adequate 1-dof devices. Such a serial combination is the mostly adopted configuration in biology (arms and legs) and is also well established in engineering for general purpose robots or xy-tables. This strategy is however not well adaptable when very high accuracy is demanded. It is then no longer possible to guarantee linearity and actuator alignment. Crosstalk also appears and the system's stiffness is no longer sufficient. Another way of achieving good accuracy is the compensation of predictable and unpredictable errors by means of an external sensor. Systematic as well as random errors can then be compensated for by a closed loop control. As a consequence, ultra accurate positioning devices are no longer needed.

Considering the need for high resonant frequencies and compactness in micropositioning, parallel mechanisms seem to be well adapted. Exactly this structure was used for the development of *Abalone*, a fully parallel planar 3-dof mechanism⁷

3.1. Design

Abalone consists basically of two platforms connected by three preloaded piezo stack-actuators between elastic joints (Fig. 2). This body is cut out of a single piece by wire electro erosion. The actuators are pressed into the steel body with an excess of 4 μm at room temperature. This way of fixing the piezo elements is on the one hand very compact and there is no need for screws or glue, which certainly would decrease the system's quality and its strength. On the other hand it allows a built-in preload that is necessary to transmit tension loads.

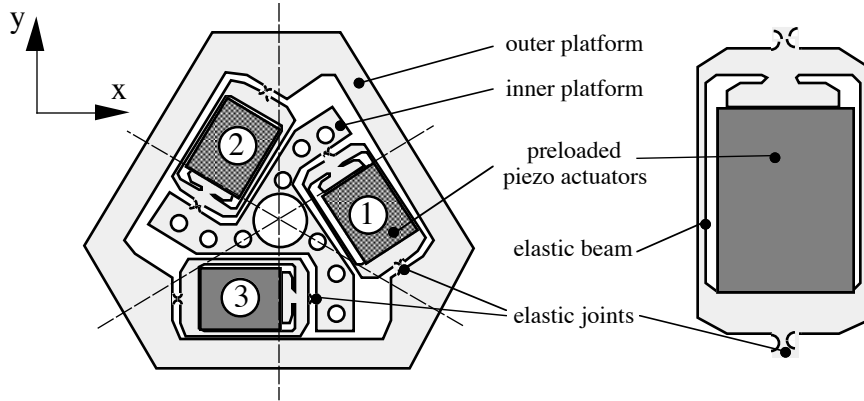


Fig. 2: Sketch of *Abalone* and detail of the actuator

The inner platform ($m_1 = 15.2 \text{ g}$) rests on the ground through three ruby-sphere feet. The outer one ($m_2 = 42.0 \text{ g}$) serves as an inertial mass and will carry a table or a tool. Supplied with appropriate voltages $U = [U_1, U_2, U_3]^T$ the actuators are able to move the outer platform in the three (planar) directions. The linearized geometric relation between the link extensions $q = [q_1, q_2, q_3]^T$ and the position of the moving platform's center $X = [x, y, r \cdot \Theta]^T$ is expressed by

$$dQ = J^{-1} \cdot dX = \begin{bmatrix} \frac{1}{2} & -\frac{\sqrt{3}}{2} & -1 \\ \frac{1}{2} & \frac{\sqrt{3}}{2} & -1 \\ -1 & 0 & -1 \end{bmatrix} \cdot dX \quad (2)$$

where r is the distance of the actuators' center line to the mechanism's symmetry center ($r = 8.4 \text{ mm}$). Fig. 3 shows a photograph of the prototype version of *Abalone* while Tab. 1 contains some of its data.

Tab. 1: Data of *Abalone*

<ul style="list-style-type: none"> • 3 dof (x, y, rotation about z) • size: 32 x 38 x 9 mm³ • local range: 5.7 μm / 0.68 mrad @ 100 V • maximum step size: 3.4 μm / 0.4 mrad • step factors, translation: $\kappa_t = 0.73$ <li style="padding-left: 20px;">rotation: $\kappa_r = 0.81$ • speed: 1 mm/s @ 400 Hz • mass: 57 g
--

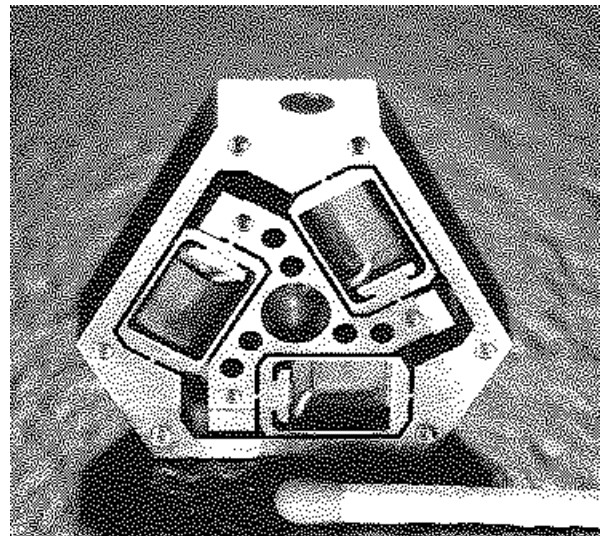


Fig.3: Prototype of *Abalone*, bottom view

3.2. Performance

Firstly, for precise movements, it is necessary to know the exact displacement of the TCP during rough motion (inertial mode). Fig. 4 shows the behaviour of Abalone at a peak-to-peak voltage of $U = 80V \cdot [1, -1, 0]$, which results in a movement in the y -direction of $2.7 \mu\text{m}/\text{step}$ with $\kappa_t = 0.73$ found theoretically from equation (1). The experimental value of $\Delta x/d = 0.74$ shows very good correspondence with the theory.

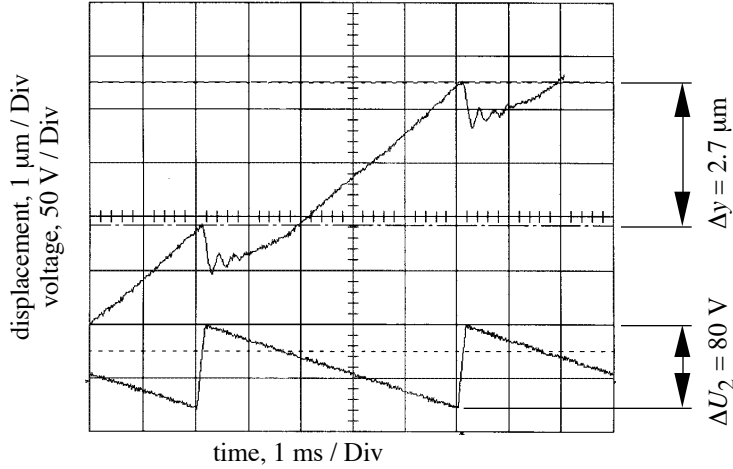


Fig. 4: Abalone's motion along the y -direction @ $f = 200 \text{ Hz}$, $V_{pp} = 80 \text{ V}$

There are, however, two remarkable patterns in Abalone's displacement: Firstly, there is a noticeable oscillation at a frequency of 3 kHz after each step. As can be seen, at step repetition rates of 500 Hz or lower this vibration fades out long before the next step arises. and does not disturb the mechanism's behaviour significantly. Secondly, the TCP's (outer platform) motion suffers from jerks of about $0.5 \mu\text{m}$, since the inner mass m_I cannot be brought to zero. In order to examine the effect of this discontinuous displacement, we put diamond crystals of the size of $100 \mu\text{m}$ onto the table and performed several movements with various speed, step size and direction and didn't notice any shift of the micro-octahedrons. If there is a need for decreasing these jerks, one solution might be the attachment of an auxiliary, redundant actuator mechanism to compensate for the insufficiencies of the main one.

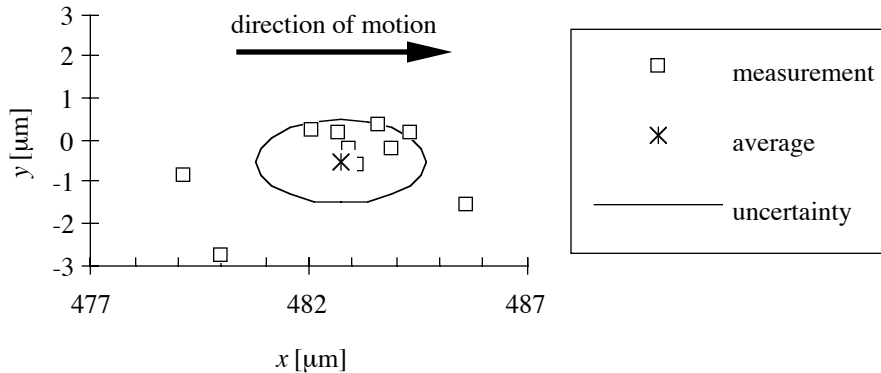


Fig. 5: Endpositions of 0.5 mm -open-loop movements

Since inertial drives are known for their poor repeatability, sensor feedback has to be implemented in order to reach the desired accuracy all over the working range. However, the open loop error is lower than 1% of the desired displacement. Fig. 5 shows the endposition of 10 $500\text{-}\mu\text{m}$ -movements in Abalone's x -direction recorded by a calibrated vision system. We can see an excellent repeatability of better than $4 \mu\text{m}$ for each endposition and an even better standard deviation (see uncertainty ellipsoid), on the other hand, there is a systematic error of about $17 \mu\text{m}$, which can be eliminated with calibration and improved physical models (piezo's hysteresis, elastic model and friction).

Fine motion control has been performed with a laser interferometer in one direction only. The accuracy achieved was 10 nm. Further efforts are being made to implement vision feedback in 3 dof under a microscope.

4. NANOCRAB - A HIGH PRECISION ROTATIONAL MOTOR

Most conventional, and also micromechanical motors use rolling or gliding bearings to guide the rotor ⁸. Because of mechanical tolerances, they show a certain runout of the order of micrometers or more and are therefore not suitable for precision tasks. Since all contact pairs also suffer from static friction these motors are limited in resolution by the stick-slip effect. Exactly this phenomenon is used advantageously in the NanoCrab.

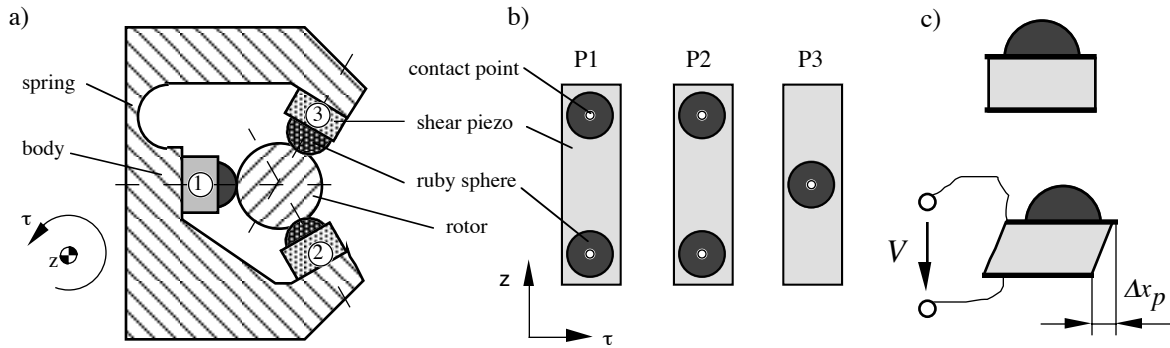


Fig. 6: NanoCrab: a) cross-section, b) contact points, c) actuator deformation

4.1. Design

A steel roller of 3 mm diameter serves as the rotor. This is practically a bearing's needle, which has the advantage of a high cylindricity (0.5 μm). It is supported by 5 ruby hemispheres glued on top of 3 shear piezo elements, as shown in Fig. 6a) and b). When a voltage V is applied to the piezo ceramics, they move the ruby-bearings tangentially to the rotor's circumference (direction τ) thereby causing rotation of the axle (Fig. 6c). Since the axle is shifted directly by the piezo-driven bearings there is no backlash or limiting static friction. The design is also very compact and simple to mount and to drive. Another advantage, compared to electromagnetic motors, is the selfstability, which offers the possibility of open loop, low-cost-control operation. Moreover, NanoCrab keeps its position, even under load, without any power consumption.

Tab.2: Data of NanoCrab

<ul style="list-style-type: none"> • size: 11 x 8 x 8 mm • rotor diameter: 3 mm • nominal step size: 0.14 mrad • angular resolution: <0.1 μrad • working frequency: 2 kHz • maximum speed (no load): 1 rpm @ 20 kHz • maximum static load: 0.92 mNm • maximum torque: 0.37 mNm @ 0.5 kHz • driving voltage V_{pp}: 270 V (±135 V) • amplifier slew rate: 70 V/μs • piezo constant d_{15}: 1.6 nm/V (PXE71)
--

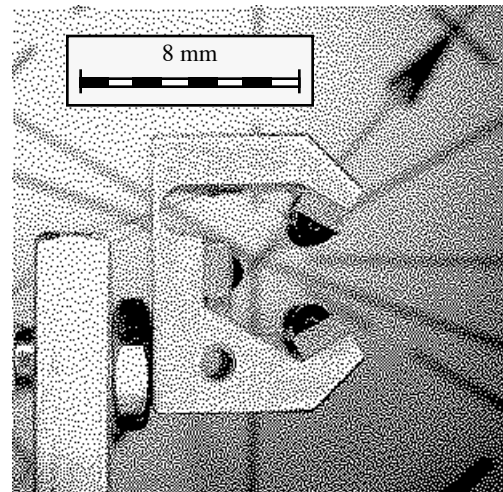


Fig.7: NanoCrab without rotor

All friction-based drives need to be preloaded (e.g. elastically or by gravitation) in order to produce sufficient tangential force at the contact points. In our prototype (Fig. 7) the normal force is supplied by a special clamp construction cut into the NanoCrab's body. It consists of a thin elastic spring and a lever and shows an overall stiffness of 31 N/mm. For fixation in the

axial direction (z) a circular V-groove is cut into the rotor's circumference. The hemispheres on top of P3 (fig. 6b) fits into this groove and prevents axial shift. Other solutions for translational holding are further axial bearings or active control with another three of piezo elements excited in the z-direction.

4.2. Performance

NanoCrab's speed strongly depends on the load torque M and sum of the preloads F_N acting at the contact points. Büchi⁶ formulates the step size Δx as the difference between an ideal piezo's displacement Δx_p (zero load deformation Δx_{p0} (3) minus elastic deformation Δx_{el} (4)) and the "lost motion" Δx_l due to finite sawtooth fall times (5).

$$\Delta x_{p0} = d_{15} \cdot V_{pp}, \tag{3}$$

$$\Delta x_{el} = r \cdot \frac{\Delta M}{k_{el}} = (F_N \cdot r \cdot \mu + M) \cdot \frac{r}{k_{el}} \tag{4}$$

$$\Delta x_l = r \cdot \omega \cdot T_f^2 = r \cdot \frac{F_N \cdot r \cdot \mu + M}{I} \cdot T_f^2 \tag{5}$$

The step size at the rotor's circumference can be written as

$$\begin{aligned} \Delta x &= \Delta x_p - \Delta x_l = (\Delta x_p - \Delta x_{el}) - \Delta x_l = \\ &= d_{15} \cdot V_{pp} - r \cdot (F_N \cdot r \cdot \mu + M) \cdot \left(\frac{T_f^2}{I} + \frac{1}{k_{el}} \right) \end{aligned} \tag{6}$$

where r is the rotor radius, ΔM the difference of friction torque before and during the step, k_{el} the structure's rotational elastic spring constant, μ the coefficient of friction, ω the rotor's speed, I the rotor's inertia and T_f the fall time of the driving voltage. This relation is valid as long as IM is smaller than the frictional torque ($F_N r \mu$) and Δx_l is smaller than Δx_p .

Static measurements showed a correlation between the frictional torque and the preload mass of 5.1 mNm/kg (Fig. 8, static). In theory, under ideal conditions, the maximum dynamic torque (operation) should reach the static (holding) torque. Due to the voltage function's finite fall time, surface effects and vibrations etc. NanoCrab only reaches 35 % of this value (Fig. 8, dynamic).

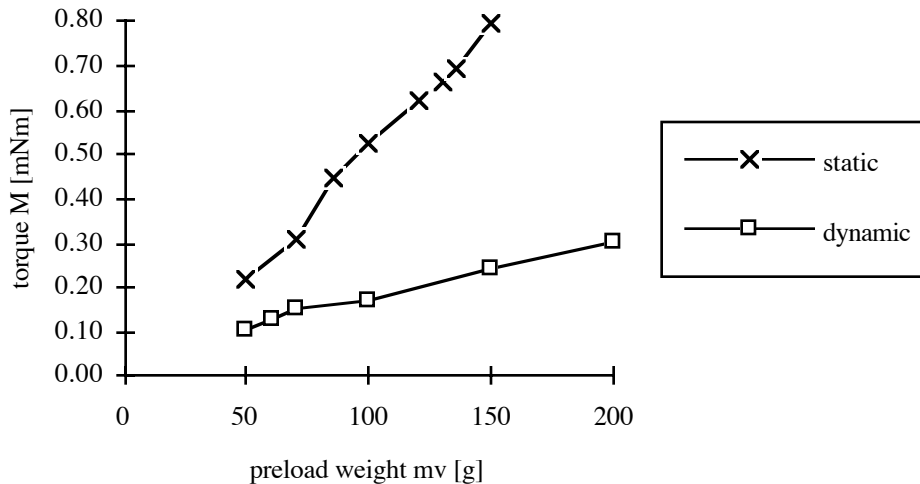


Fig.8: NanoCrab's maximum output torque @ $f = 1$ kHz, $V_{pp} = 200$ V

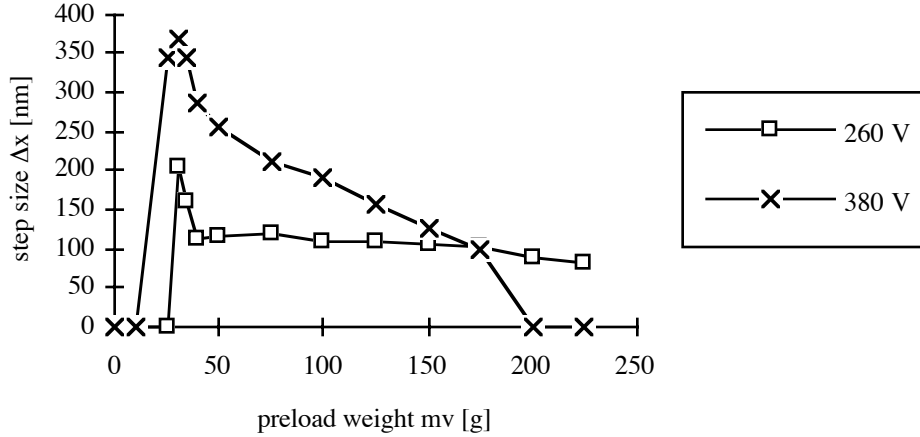


Fig.9: NanoCrab's step size @ $f = 1$ kHz, $M = 0$

Equation (6) states a strong interaction firstly between F_N and Δx (Fig. 9) and M on the other hand (Fig. 8): As F_N is increased, Δx becomes smaller, but the motor can drive heavier loads. This correlation offers the possibility of adjusting NanoCrab's "impedance" to the task within a certain range. Limiting factors are the stability ($F_N \rightarrow 0$) and parasitic vibrations, the structure's finite stiffness and the stick effect described by equation (3) (F_N large).

In the motor's present condition the preload is determined by the elastic spring system and therefore cannot be controlled actively. As a compromise, to moderate speed and high load capability, a force equivalent to a 150 g preload weight was chosen. The resulting operational characteristics are presented and compared to the analytical model (7) in Fig. 10 for zero load ($M = 0$).

$$\Delta x = d_{15} \cdot V_{pp} - r \cdot (F_N \cdot r \cdot \mu) \cdot \left(\frac{T_f^2}{I} + \frac{1}{k_{el}} \right) = d_{15} \cdot V_{pp} - r \cdot M_{\mu} \cdot \left(\frac{T_f^2}{I} + \frac{1}{k_{el}} \right) \quad (7)$$

With the current implementation, the parameters are: $d_{15} = 1.6$ nm/V, $M_{\mu} = 0.92$ Nmm (friction torque, gained from static measurements), $r = 1.5$ m. Since the electronic amplifier limits the maximum voltage slope, the fall time T_f increases from 2 μ s @ 150 V to 5.5 μ s @ 270 V.

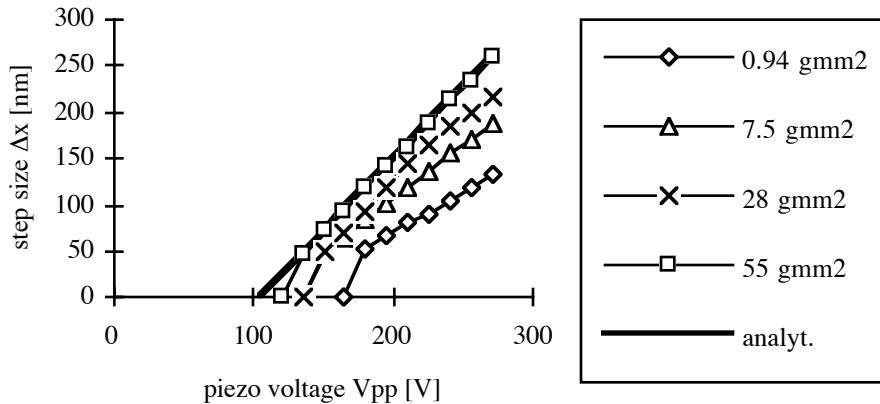


Fig.10: The characteristics of the analytical model and the real system

For large inertial values the term with T_f^2 is neglectable and therefore the only term depending on the voltage in (7) is the piezo displacement $d_{15} \cdot V_{pp}$. Fig. 10 shows the excellent correspondence between theory and measurement for inertias larger than 10 gmm^2 . The effective d_{15} can be determined as 1.6 nm/V, which is three times higher than specified in PXE71-data sheets⁹. It is

also apparent that there is a voltage V_{min} for each value of inertia beyond which the NanoCrab does not rotate. This minimum input depends strongly on the friction torque caused by the preload and the motor's elasticity. For an infinite inertia it can be written as

$$V_{min} = \frac{M_{\mu} \cdot r}{k_{el} \cdot d_{15}} \tag{8}$$

Because the spring constant is difficult to calculate or measure, it is estimated roughly from Fig 10. ($V_{min} = 105$ V for $I \rightarrow \infty$) and (8) as 19 Nm/rad. It should also be mentioned that the step size decreases again for values of inertia higher than 100 gmm². Although, at present this phenomenon is not exactly understood, we blame resonance effects due to the heavier masses for the unexpected behaviour.

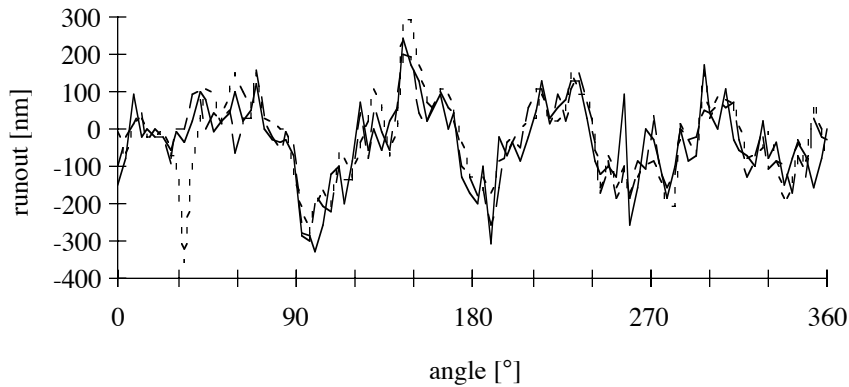


Fig.11: Runout of NanoCrab's rotor for 3 rotations

As mentioned above, the maximum runout of the rotational axes is defined by the rotor's cylindricity since it is supported kinematically exact at 5 contact points. Fig. 11 shows the runout over three full rotations measured at the symmetry plane of the NanoCrab with an interferometer to be smaller than the spherical tolerance of 0.5 μm. This center stability can easily be improved by using better axles, that is with better cylindricity or by using a feed-forward signal to compensate for the expected runout.

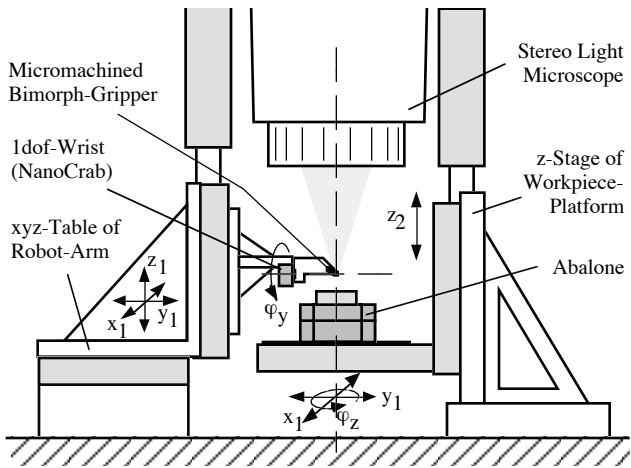


Fig.12: The ETHZ Nanorobot System containing Abalone and NanoCrab

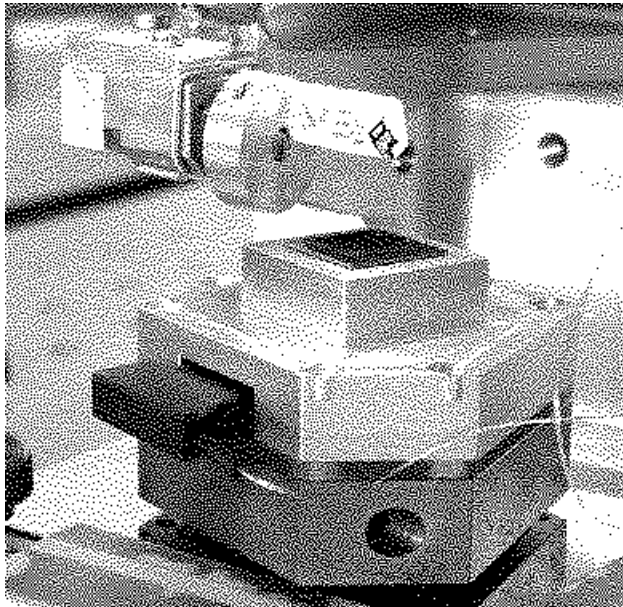


Fig.13: The Nanorobot's working area

5. IMPLEMENTATION

The current apparatus of the ETHZ-Nanorobot consists basically of two arms operating under a stereo light microscope (Fig. 12). The right arm serves as a positioning table to bring work pieces to the tool near the microscope's focus. It consists of a z-stage and Abalone and has 4 dofs. On the other hand the micromachined gripper¹⁰ is supported by an xyz-table with the NanoCrab as a wrist joint. Although the total joint space has dimension 8, the tool can be positioned relative to the work table in 5 dofs only (redundant manipulator), i.e. three translations (x, y, z) and two rotations (φ_y, φ_z). Fig. 13 shows a photograph of the robot's working area. For further information the reader can refer to ².

6. CONCLUSIONS

Two new positioning devices based on the inertial principle have been developed and have already been introduced into the ETHZ's Nanorobot System (Fig. 12).

Abalone, a planar 3-dof micro-mechanism, driven by 3 independent piezo stack actuators, serves as a very compact positioning table. In a horizontal plane, it moves its work pieces, e.g. micro diamond crystals, to the desired target with a maximum speed of 1 mm/s. In calibrated open loop operation it shows a maximum translational error of less than 1 % of the wanted displacement. When controlled with sensor feedback, the system is able to achieve an accuracy as high as Abalone's mechanical resolution of 10 nm.

On the other hand the NanoCrab, a shear piezo driven micromotor, carries the Nanorobot's tool, which is a microfabricated gripper. Since the mechanical supporting structure for the rotor serves both as a bearing and driving unit, the motor doesn't produce the stick-slip effect. Angular resolution is better than 0.1 μ rad and, at the same time, the range of rotation is theoretically infinite. Compared to electrostatic or electromagnetic motors of similar size, the device produces a relatively high torque of about 0.35 Nmm.

The performance of both Abalone and the NanoCrab, strongly depend on the load acting in the direction of the desired motion. The repeatability becomes rather poor if the counteracting impulse exceeds 10 % of the maximum load capacity. Nevertheless, the mechanisms can be fully utilised up to their capability, if a sensor feedback system is implemented and a lower speed is used.

6. REFERENCES

1. Binnig G., Rohrer H., IBM J. Res. Dev. 30, 355, 1986
2. Codourey A., Siegwart R., Zesch W., Büchi R., "A robot system for automated handling in micro-world", IROS 95 Conf. on Intell. Robots and Systems, vol. 3, pp 185-190, Aug. 1995, Pittsburgh
3. Higuchi. T., Yamagata Y., Furutani K., Kudoh K., "Precise positioning mechanisms utilising rapid deformations of piezoelectric elements", IEEE Micro Electro-mechanical Systems, 1990, Napa Valley.
4. Howald L., Rudin H., Güntherodt H.-J., "Piezoelectric inertial stepping motor with spherical rotor", Rev. Sci. Instr., 63 (8), Aug. 1992.
5. Pohl D.W., Dynamic piezoelectric translation devices, Rev. Sci. Instr., vol. 58 (1), pp54-57, Jan. 1987.
6. Büchi R., Zesch W., Codourey A., Siegwart R., "Inertial drives for micro- and nanorobots: An analytical study", SPIE Conf. on Microrobots and micromechanical systems, Oct. 1995, Philadelphia.
7. Hunt K.H., "Structural kinematics of in-parallel-actuated robot-arms", Journal of Mechanisms, Transmissions and Automation in Design, vol. 105, pp 705-712, Dec. 1983.
8. Bexell M., Johansson S., "A high torque miniature inchworm motor", Int. Conf. on Solid-State Sensors and Actuators Eurosensors IX, News, pp 69-70, June 1995, Stockholm
9. Phillips ceramic components, Designer's guide.
10. Greitmann G., Buser R., Tactile microgripper for automated handling of microparts, Transducer '95 - Eurosensors IX, June 1995, Stockholm